Self-Phase Modulation and Spectral Broadening of Optical Pulses in Semiconductor Laser Amplifiers

GOVIND P. AGRAWAL, SENIOR MEMBER, IEEE, AND N. ANDERS OLSSON

Abstract—**Amplification of ultrashort optical pulses in semiconductor laser amplifiers is shown to result in considerable spectral broadening and distortion as a result of the nonlinear phenomenon of self-phase modulation (SPM). The physical mechanism behind SPM is gain saturation which leads to intensity-dependent changes in the refractive index in response to variations in the carrier density. The effect of the shape and the initial frequency chirp of input pulses on the shape and the spectrum of amplified pulses is discussed in detail. Particular attention is paid to the case in which the input pulsewidth is comparable to the carrier lifetime so that the saturated gain has time to recover partially before the trailing edge of the pulse arrives. The experimental results, performed by using picosecond input pulses from a 1.52 μm mode-locked semiconductor laser, are in agreement with the theory. When the amplified pulse is passed through a fiber, it is initially compressed because of the frequency chirp imposed on it by the amplifier. This feature can be used to compensate for fiber dispersion in optical communication systems.**

I. INTRODUCTION

CONSIDERABLE attention has recently focused on semiconductor laser amplifiers and their potential use in optical communication systems [1], [2]. The most promising candidate for such applications is the traveling-wave optical amplifier in which the facet reflectivities of a semiconductor laser are reduced below 0.1 percent by the use of antireflection coatings. Because of an exceptionally large bandwidth (~ 5 THz), such amplifiers can amplify optical pulses as short as a few picoseconds [3]–[7]. If the amplification process were a linear process, the amplified pulse would be a replica of the input pulse as long as the amplifier bandwidth exceeds the spectral width of the input pulse. In practice, gain-saturation-induced nonlinearities lead to pulse distortion in any amplifier simply because the leading pulse edge saturates the amplifier and reduces the gain available for the trailing edge [8]–[16]. Nonetheless, the input pulse can be amplified without significant distortion if the pulse energy is a small fraction of the saturation energy. This has indeed been observed in the recent experiments [3]–[7] where pulses as short as 3 ps have been amplified without much distortion. In the saturation regime both pulse compression and pulse broadening have been observed [5] depending on the operating conditions. Extensive numerical models have been developed to study pulse-shaping effects in semiconductor laser amplifiers [17]–[19].

In most of the experiments dealing with the amplification of ultrashort pulses in semiconductor laser amplifiers [3]–[7] the spectral characteristics of the amplified pulse have not been investigated. Even when the pulse shape remains nearly unchanged during the amplification process, the pulse spectrum can be distorted considerably if the refractive index becomes nonlinear [13]. This is particularly important for semiconductor laser amplifiers where the changes in the carrier density occurring as a result of gain saturation invariably lead to relatively-large changes in the refractive index. Indeed, in a recent experiment [20] we found that the pulse spectrum shifted toward the long-wavelength side (the red shift) and contained considerable internal structure. The spectral shift depended on the input pulse energy and the amplifier gain, among other things, and was ~ 100 GHz for 10 ps pulses. The physical mechanism behind the spectral shift and distortion is the self-phase modulation (SPM) occurring as a result of index nonlinearities induced by gain saturation.

The objective of this paper is to investigate in detail how gain saturation in semiconductor laser amplifiers affects the shape and the spectrum of the optical pulse being amplified. In Section II we obtain the basic equations which govern the dynamics of the amplification process while indicating clearly the approximations made in their derivation. These equations are solved in a closed form in Section III for the case in which the input pulses are much shorter than the carrier lifetime τ_c. Section IV describes how the pulse shape and the spectrum depend on the shape of the input pulse. Particular attention is paid to the SPM-induced frequency chirp imposed by the amplifier as the pulse is amplified. The effect of an initial chirp on the input pulse is also discussed in this section. Section V extends the theory to the case in which the width τ_p of the input pulse becomes comparable to the carrier lifetime τ_c so that the saturated gain has time to recover partially. The quasi-CW limit ($\tau_p >> \tau_c$) is also considered to emphasize that SPM-induced spectral broadening occurs even for relatively long pulses. The experimental results are presented in Section VI, where we discuss how the amplifier-induced chirp can be useful for optical communication systems. The main results of the paper are summarized in Section VII.

Manuscript received February 7, 1989; revised May 31, 1989. The portion of this work performed at the University of Rochester was supported in part by the Joint Services Optics Program.

G. P. Agrawal is with the Institute of Optics, University of Rochester, Rochester, NY 14627.

N. A. Olsson is with AT&T Bell Laboratories, Murray Hill, NJ 07974.

IEEE Log Number 8930609.

II. Basic Equations

The theory of pulse propagation in amplifiers is well known [8]–[16]. It generally treats the amplifier as a two-level system, an approach suitable for gaseous and solid-state amplifiers. It can be extended for semiconductor laser amplifiers if the active region is modeled as a collection of noninteracting two-level systems with transition energies extending over the whole range of the conduction and valence bands. Such an approach is, however, too cumbersome to be useful. Considerable simplification occurs if the pulse width τ_p is assumed to be much larger than the intraband relaxation time τ_{in} that governs the dynamics of the induced polarization. Since τ_{in} is typically 0.1 ps or less, the assumption holds well for $\tau_p \geq 1$ ps. In this rate-equation approximation, the medium response to the optical field $\boldsymbol{E}$ is described by the carrier-density rate equation [21]

$$\frac{\partial N}{\partial t} = D\nabla^2 N + \frac{I}{qV} - \frac{N}{\tau_c} - \frac{a(N - N_0)}{\hbar\omega_0} |\boldsymbol{E}|^2 \quad (2.1)$$

where N is the carrier density (for electrons as well as holes), D is the diffusion coefficient, I is the injection current, q is the electron charge, V is the active volume, τ_c is the spontaneous carrier lifetime, $\hbar\omega_0$ is the photon energy, a is the gain coefficient, and N_0 is the carrier density required for transparency.

The propagation of the electromagnetic field inside the amplifier is governed by the wave equation

$$\nabla^2 \boldsymbol{E} - \frac{\epsilon}{c^2} \frac{\partial^2 \boldsymbol{E}}{\partial t^2} = 0 \quad (2.2)$$

where c is the velocity of light. The dielectric constant ϵ is given by

$$\epsilon = n_b^2 + \chi \quad (2.3)$$

where the background refractive index n_b is generally a function of the transverse coordinates x and y to account for the dielectric waveguiding in semiconductor laser amplifiers. The susceptibility χ represents the contribution of the charge carriers inside the active region of the amplifier and is a function of the carrier density N. The exact dependence of χ on N is quite complicated as it depends on details of the band structure (among other things). A simple phenomenological model has been found quite useful in the theory of semiconductor lasers [21]. In this model, χ is assumed to depend on the carrier density N linearly and is given by

$$\chi(N) = -\frac{\bar{n}c}{\omega_0}(\alpha + i)a(N - N_0) \quad (2.4)$$

where $\bar{n}$ is the effective mode index. The carrier-induced index change, responsible for SPM, is accounted for through the parameter α that is sometimes called the linewidth enhancement factor [22], [23]. Its typical values for semiconductor lasers and optical amplifiers are in the range 3–8. It should be stressed that α is expected to vary from amplifier to amplifier and should be determined independently for a comparison between theory and experiment.

Equations (2.1)–(2.4) provide a general theoretical framework for the propagation of optical pulses in semiconductor laser amplifiers. In practice, it is necessary to make several simplifying approximations. We consider an ideal traveling-wave amplifier and assume that the active-region dimensions are such that the amplifier supports a single waveguide mode. Assuming that the input light is linearly polarized and remains linearly polarized during propagation, the electric field inside the amplifier can be written as

$$\boldsymbol{E}(x, y, z, t) = \hat{x}\,\tfrac{1}{2}\left\{F(x, y)A(z, t) \cdot \exp\left[i(k_0 z - \omega_0 t)\right] + \text{c.c.}\right\} \quad (2.5)$$

where $\hat{x}$ is the polarization unit vector, $F(x, y)$ is the waveguide-mode distribution, $k_0 = \bar{n}\omega_0/c$, and $A(z, t)$ is the slowly-varying envelope associated with the optical pulse. If we substitute (2.5) in (2.2), neglect the second derivatives of $A(z, t)$ with respect to z and t, and integrate over the transverse dimensions, we obtain

$$\frac{\partial^2 F}{\partial x^2} + \frac{\partial^2 F}{\partial y^2} + (n_b^2 - \bar{n}^2)\frac{\omega_0^2}{c^2} F = 0 \quad (2.6)$$

$$\frac{\partial A}{\partial z} + \frac{1}{v_g}\frac{\partial A}{\partial t} = \frac{i\omega_0 \Gamma}{2\bar{n}c}\chi A - \frac{1}{2}\alpha_{\text{int}} A \quad (2.7)$$

where the group velocity $v_g = c/n_g$, the group index $n_g = \bar{n} + \omega_0(\partial\bar{n}/\partial\omega)$, and the confinement factor

$$\Gamma = \int_0^w \int_0^d |F(x, y)|^2\, dx\, dy \Big/ \int_{-\infty}^{\infty} \int |F(x, y)|^2\, dx\, dy. \quad (2.8)$$

The solution of (2.6) provides the transverse distribution $F(x, y)$ and the effective mode index $\bar{n}$. Equation (2.7) governs the evolution of the pulse amplitude along the amplifier length. The transverse effects are included through the confinement factor Γ. The last term in (2.7) takes into account the internal loss α_{int} experienced by the mode when $\chi = 0$. The group-velocity dispersion related to $\partial^2\bar{n}/\partial\omega^2$ is neglected since its effect on pulse propagation is negligible for typical amplifier lengths ($L = 0.2$ to 0.5 mm) and pulsewidths ($\tau_p \gtrsim 1$ ps). It can be included by adding a term containing $\partial^2 A/\partial t^2$ on the left-hand side of (2.7).

The carrier-density equation (2.1) can also be simplified by noting that the width w and the thickness d of the active region are generally smaller while the amplifier length is much larger than the diffusion length. Since the carrier density is nearly uniform along the transverse dimensions, we can use an average value, to a good approximation, and neglect carrier diffusion. By averaging (2.1) over the active-region dimensions, we obtain

$$\frac{\partial N}{\partial t} = \frac{I}{qV} - \frac{N}{\tau_c} - \frac{g(N)}{\hbar\omega_0}|A|^2 \quad (2.9)$$

where the gain is defined by

$$g(N) = \Gamma a(N - N_0). \tag{2.10}$$

It is convenient to combine (2.9) and (2.10) and obtain

$$\frac{\partial g}{\partial t} = \frac{g_0 - g}{\tau_c} - \frac{g|A|^2}{E_{\text{sat}}} \tag{2.11}$$

where E_{sat} is the saturation energy of the amplifier

$$E_{\text{sat}} = \hbar\omega_0\sigma/a \tag{2.12}$$

and σ is the mode cross-section ($\sigma = wd/\Gamma$). The small-signal gain is defined by

$$g_0 = \Gamma a N_0(I/I_0 - 1) \tag{2.13}$$

where $I_0 = qVN_0/\tau_c$ is the current required for transparency. In (2.11), A is normalized such that $|A|^2$ represents the power. The saturation energy E_{sat} determines the pulse energy above which the amplifier is heavily saturated. Typically $E_{\text{sat}} = 5$–10 pJ for index-guided semiconductor laser amplifiers [4].

Equations (2.7) and (2.11) govern pulse propagation in semiconductor laser amplifiers. They can be further simplified by making the transformation

$$\tau = t - z/v_g \tag{2.14}$$

where the reduced time τ is measured in a reference frame moving with the pulse. It is also useful to separate the amplitude and phase of the pulse by using

$$A = \sqrt{P}\exp(i\phi) \tag{2.15}$$

where $P(z, \tau)$ and $\phi(z, \tau)$ are the power and the phase. Equations (2.7) and (2.11) together with (2.4) and (2.10) then lead to the following set of three equations:

$$\frac{\partial P}{\partial z} = (g - \alpha_{\text{int}})P \tag{2.16}$$

$$\frac{\partial \phi}{\partial z} = -\frac{1}{2}\alpha g \tag{2.17}$$

$$\frac{\partial g}{\partial \tau} = \frac{g_0 - g}{\tau_c} - \frac{gP}{E_{\text{sat}}}. \tag{2.18}$$

Equation (2.17) shows the origin of SPM. The time dependence of the saturated gain $g(z, \tau)$ leads to a temporal modulation of the phase, i.e., the pulse modulates its own phase as a result of gain saturation.

III. General Solution

The evolution of the pulse inside the amplifier generally requires a numerical solution of (2.16)–(2.18). However, if $\alpha_{\text{int}} \ll g$, it is possible to solve these equations in a closed form. This condition is often satisfied in practice. In the following, we set $\alpha_{\text{int}} = 0$. Equations (2.16) and (2.17) are then readily integrated over the amplifier length to provide

$$P_{\text{out}}(\tau) = P_{\text{in}}(\tau)\exp[h(\tau)] \tag{3.1}$$

$$\phi_{\text{out}}(\tau) = \phi_{\text{in}}(\tau) - \tfrac{1}{2}\alpha h(\tau) \tag{3.2}$$

where $P_{\text{in}}(\tau)$ and $\phi_{\text{in}}(\tau)$ are the power and phase of the input pulse. The function $h(\tau)$ is defined by

$$h(\tau) = \int_0^L g(z, \tau)\, dz. \tag{3.3}$$

Physically, it represents the integrated gain at each point of the pulse profile. If we integrate (2.18) over the amplifier length and make use of (2.16) to eliminate the product gP, $h(\tau)$ is the solution of the following ordinary differential equation:

$$\frac{dh}{d\tau} = \frac{g_0 L - h}{\tau_c} - \frac{P_{\text{in}}(\tau)}{E_{\text{sat}}}[\exp(h) - 1]. \tag{3.4}$$

For a given input pulse shape $P_{\text{in}}(\tau)$ and the gain $g_0 L$, (3.4) can be solved to obtain $h(\tau)$. The output pulse shape is then obtained from (3.1). Equation (3.2) determines the phase variation of the output pulse. The pulse spectrum is obtained by using

$$S(\omega) = \left| \int_{-\infty}^{\infty} [P_{\text{out}}(\tau)]^{1/2} \cdot \exp[i\phi_{\text{out}}(\tau) + i(\omega - \omega_0)\tau]\, d\tau \right|^2. \tag{3.5}$$

Equation (3.4) can be solved analytically in one important case. If the input pulsewidth τ_p is much smaller than the carrier lifetime τ_c, the first term on the right-hand of (3.4) can be neglected. Physically, its neglect amounts to assuming that the pulse is so short that the gain has no time to recover. Typically, $\tau_c = 0.2$–0.3 ns for semiconductor laser amplifiers, and the above approximation holds well for $\tau_p < 50$ ps. In the limit $\tau_p/\tau_c \ll 1$, the solution of (3.4) is [16]

$$h(\tau) = -\ln\left[1 - \left(1 - \frac{1}{G_0}\right)\exp\left(-\frac{U_{\text{in}}(\tau)}{E_{\text{sat}}}\right)\right] \tag{3.6}$$

where $G_0 = \exp(g_0 L)$ is the unsaturated single-pass amplifier gain and

$$U_{\text{in}}(\tau) = \int_{-\infty}^{\tau} P_{\text{in}}(\tau')\, d\tau'. \tag{3.7}$$

The quantity $U_{\text{in}}(\tau)$ represents the fraction of the pulse energy contained in the leading part of the pulse up to $\tau' \le \tau$. By definition, $U_{\text{in}}(\infty) = E_{\text{in}}$, where E_{in} is the input pulse energy. As an example, consider a Gaussian pulse for which

$$P_{\text{in}}(\tau) = \frac{E_{\text{in}}}{\tau_0\sqrt{\pi}}\exp\left(-\frac{\tau^2}{\tau_0^2}\right) \tag{3.8}$$

where τ_0 is related to the full width at half maximum (FWHM) by $\tau_p \simeq 1.665\,\tau_0$. By using (3.8) in (3.7)

$$U_{\text{in}}(\tau) = \tfrac{1}{2}E_{\text{in}}[1 + \text{erf}(\tau/\tau_0)] \tag{3.9}$$

where erf stands for the error function. Equations (3.6) and (3.9) determine $h(\tau)$ for a Gaussian pulse.

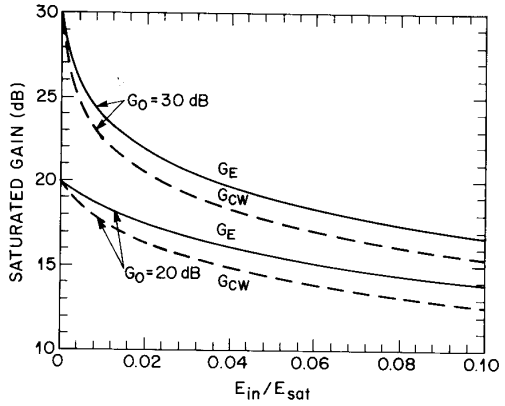

Fig. 1. Saturation characteristics of semiconductor laser amplifiers under pulsed and CW operation. Solid and dashed curves show respectively the energy gain G_E and the CW power gain G_{CW} for G_0 = 20 dB and 30 dB. The x axis corresponds to P_{in}/P_{sat} in the case of dashed curves.

The instantaneous amplifier gain $G(t)$ is determined from (3.1) and (3.6) and is given by

$$G(\tau) = \exp\left[h(\tau)\right] = \left\{1 - (1 - 1/G_0) \cdot \exp\left[-U_{in}(\tau)/E_{sat}\right]\right\}^{-1}. \quad (3.10)$$

The leading-edge gain $G(-\infty) = G_0$, as the amplifier is not yet saturated. The trailing-edge or the final gain G_f is obtained by setting $\tau = \infty$ in (3.10) and is given by

$$G_f = G(\infty) = \frac{G_0}{G_0 - (G_0 - 1)\exp\left(-E_{in}/E_{sat}\right)}. \quad (3.11)$$

The quantity of practical interest is the energy gain defined as

$$G_E = \frac{E_{out}}{E_{in}} = \frac{1}{E_{in}} \int_{-\infty}^{\infty} P_{in}(\tau) \exp\left[h(\tau)\right] d\tau \quad (3.12)$$

where we used (3.1) to obtain the energy of the output pulse. The energy gain can be expressed in terms of G_0 and G_f by using (3.6) and is given by [16]

$$G_E = \frac{\ln\left[(G_0 - 1)/(G_f - 1)\right]}{\ln\left[(G_0 - 1)/(G_f - 1)\right] - \ln\left(G_0/G_f\right)}. \quad (3.13)$$

It is interesting to note that the energy gain is independent of the input pulse shape.

Fig. 1 shows how the energy gain decreases with an increase in the input pulse energy for G_0 = 20 and 30 dB. The curves characterize the saturation characteristics of the amplifier under pulsed operation such that $\tau_p << \tau_c$. For comparison, the CW-saturation characteristics are also shown in Fig. 1. The CW power gain G_{CW} is obtained by using the steady-state solution of (2.18) given by

$$g = g_0/(1 + P/P_{sat}) \quad (3.14)$$

in (2.16). Here $P_{sat} = E_{sat}/\tau_c$ is the saturation power. For $\alpha_{int} = 0$, the CW power gain is given by

$$G_{CW} = G_0 \exp\left[-(G_{CW} - 1)P_{in}/P_{sat}\right]. \quad (3.15)$$

Fig. 1 shows that the energy gain saturates slower than the CW power gain. The input pulse energy corresponding to 50 percent (3 dB) reduction in the unsaturated gain G_0 depends on G_0 itself. For G_0 = 20 dB, the 3 dB saturation energy E_{in}/E_{sat} = 0.03, but becomes 0.002 for G_0 = 30 dB.

IV. Pulse Shape and Spectrum

In this section we use the solution given by (3.1) and (3.2) to study the shape and the spectrum of the amplified pulses. For the case of an unchirped (transform-limited) Gaussian input pulse, (3.6) and (3.9) provide the integrated gain $h(\tau)$. Figs. 2 and 3 show the shape and the spectrum of the amplified pulse for several values of the unsaturated amplified gain G_0. The input pulse energy corresponds to E_{in}/E_{sat} = 0.1. The linewidth enhancement factor may vary from one amplifier to another as it depends on the relative position of the gain peak with respect to the operating wavelength. We choose α = 5 as a representative value for all of our calculations. Fig. 2 shows that the amplified pulse becomes asymmetric such that its leading edge is sharper compared with the trailing edge. Sharpening of the leading edge is a common feature of all amplifiers [8]–[13] and occurs because the leading edge experiences larger gain than the trailing edge.

The pulse spectra of Fig. 3 show features which are unique to semiconductor laser amplifiers. In general, the spectrum develops a multipeak structure. The dominant spectral peak shifts to the low-frequency side (red shift). The red shift increases with the amplifier gain G_0 and can be as large as 3–5 times the spectral width of the input pulse. For 10 ps input pulses, the frequency shift can easily exceed 100 GHz. These spectral changes are due to SPM-induced frequency chirp imposed on the pulse as it propagates through the amplifier. The chirp $\Delta\nu(\tau)$ can be obtained by using the relation

$$\Delta\nu(\tau) = -\frac{1}{2\pi}\frac{\partial\phi}{\partial\tau} \quad (4.1)$$

where ϕ is the optical phase. By using (3.2) and (4.1), we obtain

$$\Delta\nu_{out}(\tau) = \Delta\nu_{in}(\tau) + \frac{\alpha}{4\pi}\frac{\partial h}{\partial\tau} \quad (4.2)$$

where $\Delta\nu_{in}$ is the frequency chirp of the input pulse if it is not transform limited. If we use $h(\tau)$ from (3.6) in (4.2), the chirp of the output pulse is given by

$$\Delta\nu_{out}(\tau) = \Delta\nu_{in}(\tau) - \frac{\alpha(G_0 - 1)}{4\pi G_0}\frac{P_{out}(\tau)}{E_{sat}} \cdot \exp\left(-\frac{U_{in}(\tau)}{E_{sat}}\right). \quad (4.3)$$

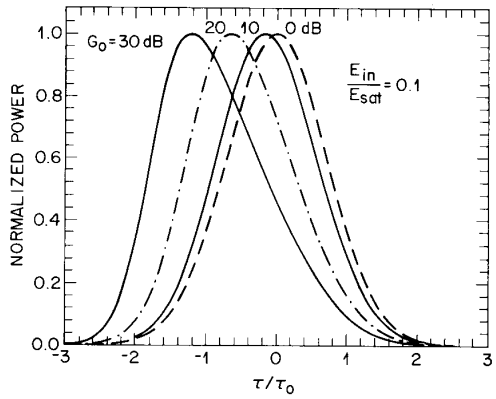

Fig. 2. Output pulse shapes for several values of the unsaturated gain G_0 when the input pulse is Gaussian with an energy such that $E_{in}/E_{sat} = 0.1$. The 0 dB curve shows the input pulse shape.

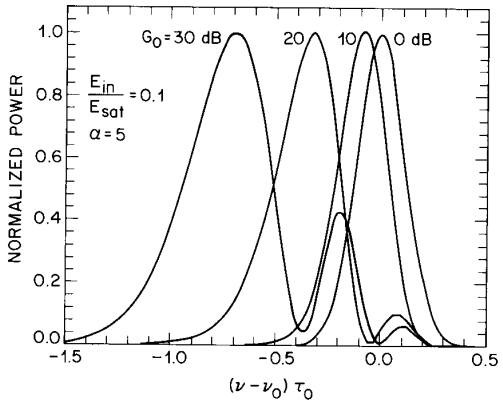

Fig. 3. Output pulse spectra corresponding to the pulse shapes of Fig. 2. Note the spectral shift toward the low-frequency side with increasing G_0.

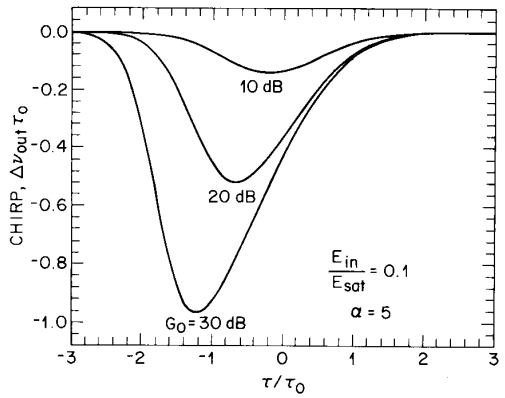

Fig. 4. Frequency chirp imposed on the output pulse during amplification of a Gaussian input pulse. The corresponding pulse shape and the spectrum are shown in Figs. 2 and 3.

Fig. 4 shows the frequency chirp across the amplified pulse for the case of an unchirped Gaussian input pulse by using parameter values identical to those used in Figs. 2 and 3. $\Delta\nu_{out}(\tau)$ is negative across the entire pulse, i.e., the instantaneous frequency is downshifted (the red shift) from the incident frequency $\nu_0 = \omega_0/2\pi$. The temporal variation of the chirp is almost identical to that of the output pulse shape (compare with Fig. 2). This is expected from (4.3) if we note that the exponential factor changes only from 1 to 0.9 across the entire pulse for $E_{in}/E_{sat} = 0.1$ and has a minor effect on the chirp profile. The structure in the pulse spectra shown in Fig. 3 results from an interference phenomenon that is common to SPM in all nonlinear media [24]. Physically, the instantaneous frequency is the same at two distinct points within the pulse profile. Depending on the relative phases of the optical fields at those two points, the fields can interfere destructively or constructively. This interference leads to an oscillatory structure in the pulse spectrum. The asymmetry is a direct consequence of the asymmetric shape of the output pulse. A noteworthy feature of the chirp profiles shown in Fig. 4 is that the chirp increases almost linearly over the central part ($|\tau| \lesssim \tau_0$) of the pulse. Such a linear chirp implies that the pulse can be compressed in a dispersive medium such as an optical fiber if it experiences anomalous group-velocity dispersion (GVD) during its propagation in that medium [25].

Although the case of an unchirped Gaussian pulse is applicable in many experimental situations, the input pulse may be far from Gaussian in some specific cases and may also have an initial chirp imposed on it. This is the case, for example, for pulses emitted by a directly modulated semiconductor laser. A super-Gaussian model can be used for studying the pulse shape effects [25], [26]. The amplitude of the input pulse in this model is given by

$$A_{in}(\tau) = \sqrt{P_{in}} \exp\left[-\frac{1+iC}{2}\left(\frac{\tau}{\tau_0}\right)^{2m}\right] \quad (4.4)$$

where P_{in} is the peak power, C is the chirp parameter, and the parameter m controls the shape of the super-Gaussian pulse. The case of a Gaussian pulse corresponds to $m = 1$. For larger values of m, the pulse becomes increasingly square shaped with sharper leading and trailing edges. If we define the rise time τ_r as the interval during which the power increases from 10 to 90 percent of its peak value, from (4.4) we obtain

$$\tau_r = \tau_0\left[(\ln 10)^{1/2m} - (\ln (10/9))^{1/2m}\right]. \quad (4.5)$$

The parameter m thus relates the rise time to the width parameter τ_0. The peak power P_{in} is related to the input pulse energy by the relation

$$E_{in} = \int_{-\infty}^{\infty} |A_{in}(\tau)|^2 \, d\tau = \frac{\tau_0}{m}\Gamma\left(\frac{1}{2m}\right) P_{in} \quad (4.6)$$

where $\Gamma(x)$ stands for the gamma function of its argument x.

Fig. 5 shows the output pulse shapes when the input pulse is an unchirped ($C = 0$) super-Gaussian pulse with $m = 3$. The input pulse energy is taken to be the same ($E_{in}/E_{sat} = 0.1$) as in Fig. 2 to facilitate comparison with the Gaussian-pulse case. The output pulse has a long tail

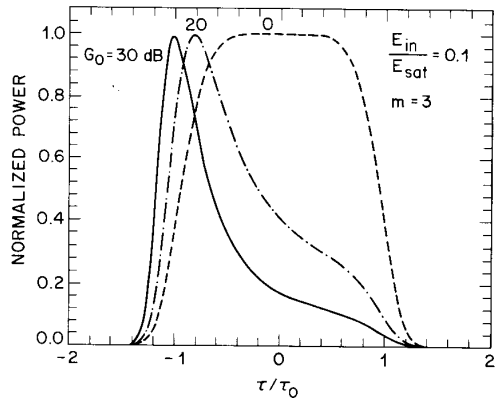

Fig. 5. Output pulse shapes for G_0 = 20 and 30 dB when the input pulse is an unchirped super-Gaussian pulse (0 dB curve). The parameters are identical to those of Fig. 2 to facilitate comparison with the Gaussian-pulse case.

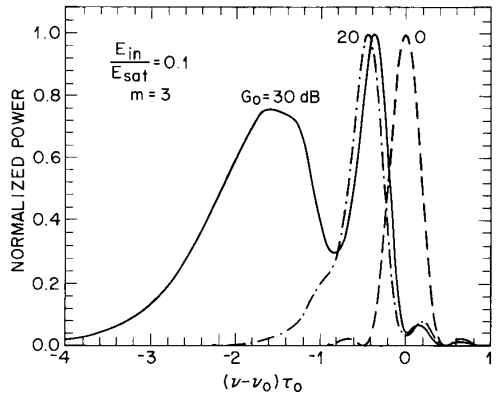

Fig. 6. Output spectra corresponding to the pulse shapes of Fig. 5. The input pulse is super-Gaussian. Compare with Fig. 3 where the Gaussian-pulse case is shown.

on the trailing edge and appears to be narrower than the input pulse on the basis of its FWHM. This is in contrast with the Gaussian-pulse case shown in Fig. 2 where the FWHM of the output pulse is larger than the input pulse. Pulse broadening as well as pulse narrowing has been observed experimentally [5]. Our theory shows that such features may be related to the shape of the input pulse.

The output spectra corresponding to the pulse shapes of Fig. 5 are shown in Fig. 6. A direct comparison of Fig. 6 with Fig. 3 shows how much spectral distortion depends on the input pulse shape. In both cases the spectrum has a multipeak structure and its shifted towards the red side. However, the amount of the shift and the amplitudes of various peaks are quite different. In particular, the output spectrum for the super-Gaussian pulse has two dominant peaks. The origin of these two peaks can be understood by considering the chirp profile of (4.3). As noted before, the chirp variation follows the output pulse shape quite closely. We can thus use Fig. 5 to understand the spectral features. The broad red-shifted peak in Fig. 6 for G_0 = 30 dB results from the huge chirp on the leading part of the output pulse. The second spectral peak contains the energy of the central and the trailing part of the pulse where the chirp is low. Note also that the chirp does not vary linearly for the super-Gaussian pulse.

The output pulse spectrum also depends on the initial chirp if the input pulses are not transform limited. Fig. 7 shows this dependence by considering the amplification of chirped Gaussian pulses (m = 1) for C = −5 and 5. The case of an unchirped Gaussian pulse (C = 0) is also shown for comparison. Depending on the sign of the chirp parameter C the spectral shift can increase or decrease from that of C = 0. The magnitude of C can be determined from the input spectral width which increases by a factor $(1 + C^2)^{1/2}$ for chirped Gaussian pulses. The sign of C depends on whether the frequency increases (C > 0) or decreases (C < 0) with time across the pulse. For C > 0, the SPM-induced chirp adds to the input-pulse chirp, and the spectrum shifts even more to the red side

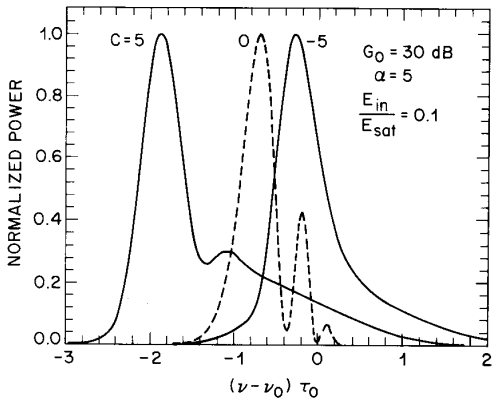

Fig. 7. Output spectra for chirped Gaussian input pulses for C = 5 and −5. The case of unchirped (C = 0) Gaussian pulses is also shown for comparison. The other parameters are identical to those of Figs. 3 and 4.

than the case when C = 0. The opposite occurs when C < 0. These features are clearly seen in Fig. 7. A qualitatively similar behavior occurs for other pulse shapes.

V. Effect of Gain Recovery

The results of Section IV are obtained by assuming that the input pulse is much shorter than the carrier lifetime ($\tau_0 \ll \tau_c$). Typically τ_c = 200 ps, and the assumption holds quite well for τ_0 up to 30 ps or for $\tau_p \leq$ 50 ps. When the pulsewidth become comparable to τ_c, the saturated gain has time to recover during the pulse. Such a partial gain recovery would affect both the shape and the spectrum of output pulses. In this section we study the effect of gain recovery on gain dynamics.

The general solution given by (3.1) and (3.2) still applies provided the first term on the LHS of (3.4) is not neglected in obtaining the integrated gain $h(\tau)$. It is not easy to solve (3.4) analytically but it can be solved numerically in a straightforward manner. By using the solution in (3.1) and (3.5), the shape and the spectrum of

the output pulses are readily obtained. Fig. 8 shows the effect of gain recovery on the output pulse shape when the input pulse is Gaussian and unchirped ($C = 0$). For $\tau_0/\tau_c = 0.01$, the pulse shape is nearly identical to that obtained by assuming an infinite carrier lifetime (no gain recovery). For $\tau_0/\tau_c = 0.5$, the output pulse becomes broader as its trailing side becomes more intense. This can be understood by noting that the saturated gain has time to recover partially by the time the trailing edge arrives. The net result of gain recovery is that the output pulse is less asymmetric and becomes broader than the input pulse. These features become even more pronounced for $\tau_0/\tau_c = 1$ in Fig. 8. The output pulse for this value of τ_0/τ_c is 50 percent broader than the input pulse. In the case shown in Fig. 8 gain recovery mainly affects the trailing edge of the pulse. Depending on the input parameters the output pulse may consist of a two-peak structure under certain conditions.

The output spectra corresponding to the pulse shapes of Fig. 8 are shown in Fig. 9. In the case of partial gain recovery, the spectral shift becomes smaller and the spectrum becomes less asymmetric. In particular, the sidebands on the blue side become more intense as the ratio τ_0/τ_c increases. In the limit $\tau_0 >> \tau_c$, the spectrum becomes symmetric as the gain recovery is complete.

We briefly consider the limiting case $\tau_0 >> \tau_c$ which corresponds to the quasi-CW operation of the amplifier. By neglecting the time derivative in (3.4), the integrated gain is given by the implicit relation

$$h(\tau) = g_0 L - \frac{P_{\text{in}}(\tau)}{P_{\text{sat}}}\left(\exp\left[h(\tau)\right] - 1\right) \quad (5.1)$$

where

$$P_{\text{sat}} = E_{\text{sat}}/\tau_c. \quad (5.2)$$

Figs. 10 and 11 show the shape and the spectrum of the output pulses for $P_{\text{in}}/P_{\text{sat}} = 0.01$ and 0.1 when an unchirped Gaussian pulse is amplified in an amplifier with $G_0 = 30$ dB. The pulse is symmetric, as expected. It is broader than the input pulse simply because the peak experiences less amplification than the wings because of gain saturation. The spectrum is symmetric and exhibits a structure that is characteristic of SPM in a medium whose refractive index is intensity dependent and has a form

$$n = n_0 + n_2|A|^2 \quad (5.3)$$

where n_2 is the nonlinearity coefficient [25]. It should be noted that symmetric SPM occurs only for slow pulses for which the fall time is much longer than the gain-recovery time.

It is useful to obtain an equivalent value of n_2 for semiconductor laser amplifiers. If we substitute (5.1) in (3.2) and neglect a constant phase shift, the amplifier-induced nonlinear phase shift becomes

$$\phi_{\text{out}}(\tau) = \frac{\alpha}{2}\frac{P_{\text{out}}(\tau) - P_{\text{in}}(\tau)}{P_{\text{sat}}} \quad (5.4)$$

where (3.1) was used. Typically $P_{\text{in}}(\tau) << P_{\text{out}}(\tau)$ under high-gain conditions. The effective n_2 is obtained by using the relation

$$\phi_{\text{out}}(\tau) = \frac{n_2\omega_0 L}{c\sigma} P_{\text{out}}(\tau) \quad (5.5)$$

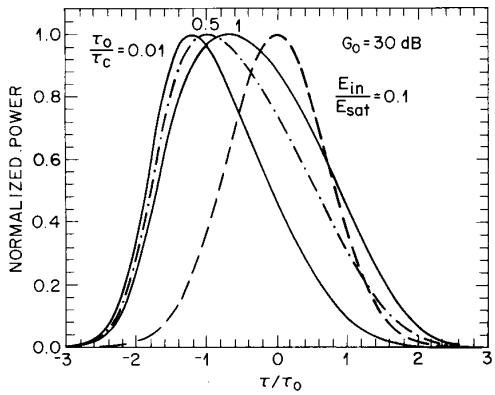

Fig. 8. Output pulse shapes for several values of τ_0/τ_c when a Gaussian input pulse (dashed curve) is amplified in an amplifier with $G_0 = 30$ dB. Changes in the pulse shape are due to partial gain recovery.

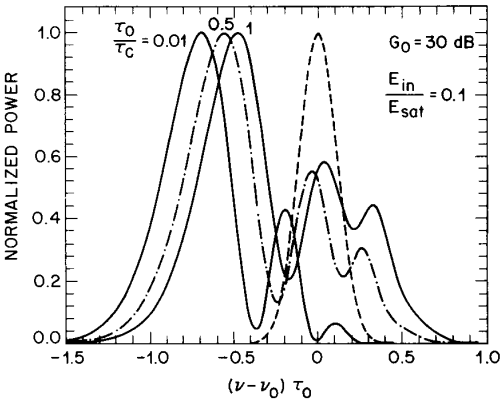

Fig. 9. Output spectra corresponding to the pulse shape of Fig. 8. The spectrum of the input Gaussian pulse is also shown for comparison by a dashed line.

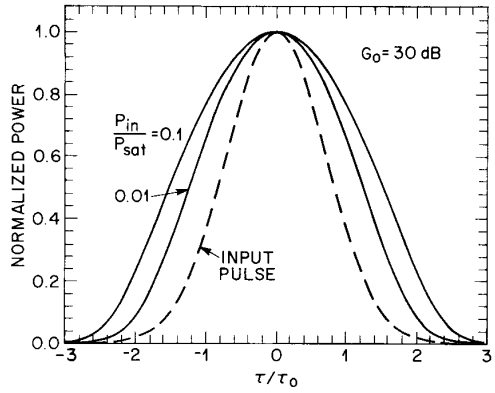

Fig. 10. Output pulse shapes in the quasi-CW limit $\tau_0 >> \tau_c$ for $G_0 = 30$ dB and $P_{\text{in}}/P_{\text{sat}} = 0.01$ and 0.1. The input Gaussian pulse is also shown in comparison.

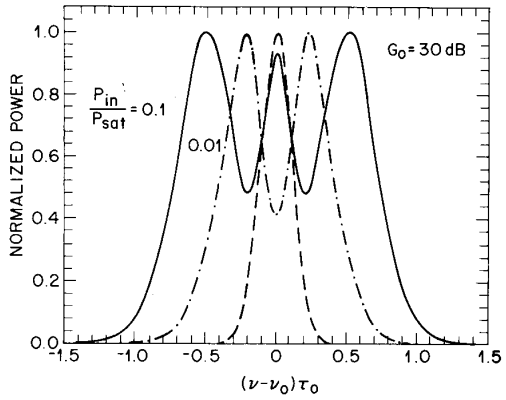

Fig. 11. Output spectra corresponding to the pulse shapes of Fig. 10. The input spectra is shown by a dashed curve for comparison.

where L is the amplifier length and $\sigma = wd/\Gamma$ is the mode cross section area. By comparing (5.4) and (5.5) and assuming $P_{in}(\tau) \ll P_{out}(\tau)$, we obtain

$$n_2 = \frac{\alpha a \tau_c c}{2\hbar\omega_0^2 L} \tag{5.6}$$

where we used (2.12) and (5.2) to express n_2 in terms of the amplifier parameters. If we use typical values $\alpha = 5$, $a = 2.5 \times 10^{-16}$ cm^2, $\tau_c = 200$ ps, $L = 250$ μm, we estimate that $n_2 \simeq 1 \times 10^{-9}$ cm^2/W. This value is quite large compared to most nonlinear media. This is why significant SPM-induced spectral broadening can occur even when the input peak powers are below 1 mW for an amplifier length of only 250 μm. Note that the nonlinearity discussed here is extrinsic in nature inasmuch as it results from the dynamic variation in the injected carrier density. As a result, the response time is determined by the carrier lifetime. The intrinsic n_2 has a fast response (because of its electronic origin), but has a value $\sim 10^{-14}$ cm^2/W. SPM due to intrinsic n_2 is negligible in semiconductor laser amplifiers because of its relatively small value.

VI. Experimental Results

Fig. 12 shows the experimental setup used to study the effect of amplification on the shape and the spectrum of picosecond optical pulses. A mode-locked external-cavity semiconductor laser operating at 1.52 μm is used as a source of picosecond pulses. The laser emits a pulse train at a repetition rate of 1 GHz. The pulsewidth can be adjusted in the range 10–60 ps. The input pulses are nearly transform limited with a time–bandwidth product of about 0.5. The laser output is coupled to a semiconductor laser amplifier through an optical isolator. The amplifier has a buried-heterostructure design, has facet reflectivities below 0.01 percent to ensure traveling-wave operation, and can provide unsaturated single-pass gains of up to 30 dB. The amplifier output is divided into two parts by using a fiber coupler. One port of the coupler is connected to a Fabry–Perot interferometer for spectral measurements while the other port is connected to a streak camera having a resolution less than 7 ps. A long piece of fiber (up to 70 km long) is inserted between the coupler and the streak camera to study pulse compression occurring as a result of the SPM-induced frequency chirp imposed by the amplifier. The single-mode fiber is the standard telecommunication type with a dispersion minimum near 1.31 μm. The fiber dispersion is about 15 ps/km/nm at 1.52 μm.

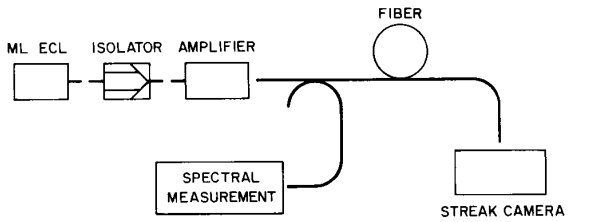

Fig. 12. Experimental setup for spectral and temporal measurements of pulses amplified by a semiconductor laser amplifier. A mode-locked external-cavity semiconductor laser (ML-ECL) is used as a source of picosecond input pulses.

Fig. 13 shows the pulse spectra at the amplifier output when 55 ps pulses having an input energy ~ 0.1 pJ are launched into the amplifier. The oscillatory structure in the observed spectra is related to the longitudinal modes of the mode-locked laser. These modes are 1 GHz apart and are resolved by the Fabry–Perot interferometer whose resolution is below 500 MHz. The pulse spectrum corresponds to the envelope of the traces shown in Fig. 13. The top trace is for an amplifier current of 34 mA. The unsaturated amplifier gain for this current is estimated to be $G_0 \simeq 10$ dB. The spectrum has a single peak and is nearly identical to the input spectrum (not shown). The bottom trace in Fig. 13 is for an amplifier current of 104 mA, a level that corresponds to $G_0 \simeq 30$ dB. The spectrum is now considerably broadened and displays a three-peak structure such that the dominant peak is shifted toward red when compared with that of the input spectrum. These features are in qualitative agreement with the theoretical spectra shown in Fig. 3.

SPM-induced spectral broadening seen in Fig. 13 is a result of the frequency chirp imposed on the pulse by the amplifier. Such a chirped pulse (see Fig. 4) can be compressed if it is passed through a dispersive delay line having anomalous dispersion. Since optical fibers exhibit anomalous dispersion near 1.52 μm, the amplified pulse would initially compress when launched into such a fiber. This feature has an important application in optical communication systems since their transmission distance can be considerably increased. To demonstrate the feasibility of such a scheme, we have propagated the amplified pulse over a 70 km long fiber. Fig. 14 shows the input pulse (trace a) and the transmitted pulse (trace b) for the case $G_0 = 30$ dB. Because of initial compression experienced by the pulse, the pulsewidth after 70 km is comparable to the input pulsewidth. By contrast, if the amplifier is operated at low gain ($G_0 < 10$ dB), the induced chirp is not large enough, and the transmitted pulse is much wider than

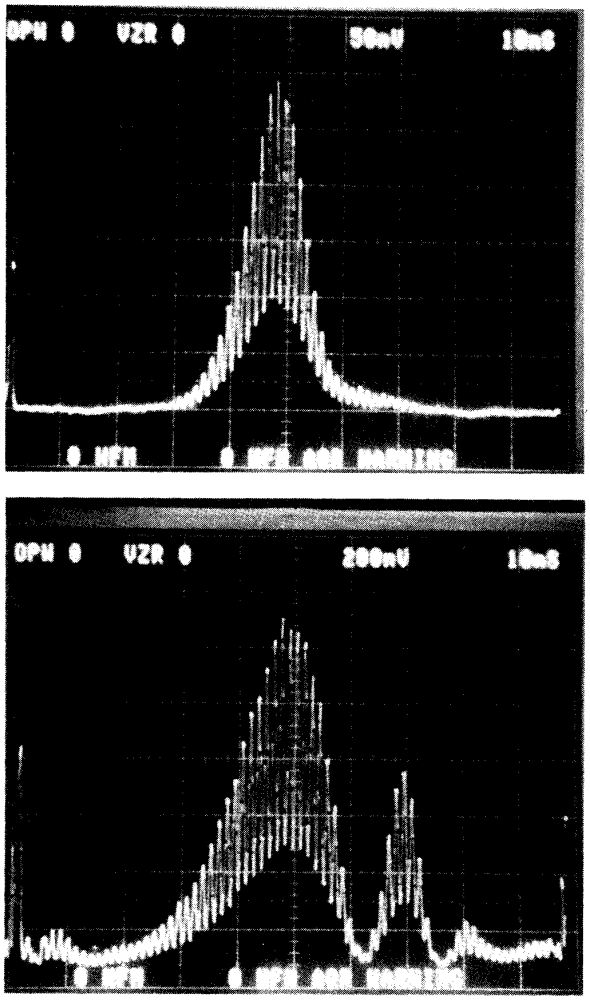

Fig. 13. Pulse spectra at the amplifier output for the case of unsaturated amplifier gain of 10 dB (upper trace) and 30 dB (lower trace).

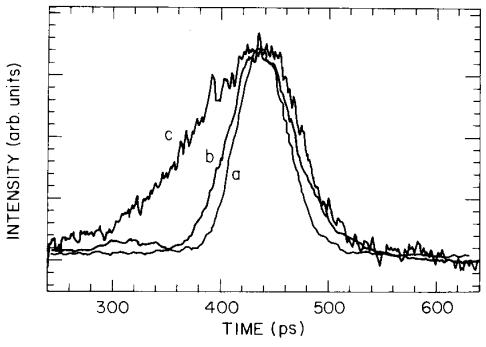

Fig. 14. Streak-camera traces of the input pulse (trace *a*) and the amplified pulse after propagating in a 70 km long fiber (trace *b*) for the case $G_0 = 30$ dB. Trace *c* shows the pulse shape when G_0 is reduced below 10 dB.

the input pulse, as evident by the trace *c* in Fig. 14. These results demonstrate that a semiconductor laser amplifier can compensate for fiber dispersion if it is operated in the saturation regime [27]. It can also be used to compress weak picosecond pulses if the fiber length is suitably optimized [28].

VII. Conclusions

This paper has presented theoretical and experimental results related to the amplification of short optical pulses in semiconductor laser amplifiers. We have identified SPM as a dominant source of spectral broadening occurring as a result of gain saturation that is responsible for time-dependent variations in the carrier density, and hence the refractive index. The temporal and spectral changes occurring during amplification depend on the relative magnitudes of the pulsewidth and the carrier lifetime. When the pulsewidth is much shorter than the carrier lifetime, both the shape and the spectrum of the amplified pulses are asymmetric. In particular, the spectrum exhibits a red shift. For input pulses longer than the carrier lifetime the spectrum is broadened on both the red and blue sides. The spectral and temporal changes also depend on the shape and the frequency chirp of the input pulses. We have analyzed the dependence on the input parameters by using a detailed theoretical model. Asymmetric SPM-induced spectral broadening has been observed experimentally. The SPM-induced frequency chirp can be used to compress the amplified pulses by passing them through a dispersive delay line. In particular, it can be used to extend the transmission distance in optical communication systems.

References

[1] M. J. O'Mahony, "Semiconductor laser optical amplifiers for use in future fiber systems," *J. Lightwave Technol.*, vol. 6, pp. 531–544, 1988, and references therein.

[2] N. A. Olsson, "Lightwave systems with optical amplifiers," *J. Lightwave Technol.*, vol. 7, pp. 1071–1092, July 1989.

[3] I. W. Marshall, D. M. Spirit, and M. J. O'Mahony, "Picosecond pulse response of a traveling-wave semiconductor laser amplifier," *Electron. Lett.*, vol. 23, pp. 818–819, 1987.

[4] J. M. Wiesenfeld, G. Eisenstein, R. S. Tucker, G. Raybon, and P. B. Hansen, "Distortionless picosecond pulse amplification and gain compression in a traveling-wave InGaAsP optical amplifier," *Appl. Phys. Lett.*, vol. 53, pp. 1239–1241, 1988.

[5] I. W. Marshall and D. M. Spirit, "Observation of large pulse compression by a saturated traveling wave semiconductor laser amplifier," *Conf. Dig. CLEO'88.* Washington, DC: Opt. Soc. Amer., 1988.

[6] M. P. Kesler and E. P. Ippen, "Subpicosecond gain dynamics in GaAlAs laser diodes," *Appl. Phys. Lett.*, vol. 51, pp. 1765–1767, 1987.

[7] G. Eisenstein, P. B. Hansen, J. M. Wiesenfeld, R. S. Tucker, and G. Raybon, "Amplification of high repetition rate picosecond pulses using an InGaAsP traveling-wave optical amplifier," *Appl. Phys. Lett.*, vol. 53, pp. 1539–1541, 1988.

[8] R. Bellman, G. Birnbaum, and W. G. Wagner, "Transmission of monochromatic radiation in a two-level system," *J. Appl. Phys.*, vol. 34, pp. 780–782, 1963.

[9] L. M. Frantz and J. S. Nodvik, "Theory of pulse propagation in a laser amplifier," *J. Appl. Phys.*, vol. 34, pp. 2346–2349, 1963.

[10] E. O. Schulz-Dubois, "Pulse sharpening and gain saturation in traveling-wave masers," *Bell Syst. Tech. J.*, vol. 43, pp. 625–658, 1964.

[11] J. P. Wittke and P. J. Warter, "Pulse propagation in a laser amplifier," *J. Appl. Phys.*, vol. 35, pp. 460–461, 1964.

[12] A. Icsevgi and W. E. Lamb, Jr., "Propagation of light pulses in a laser amplifier," *Phys. Rev.*, vol. 185, pp. 517–545, 1969.

[13] P. G. Kryukov and V. S. Letokhov, "Propagation of a light pulse in a resonantly amplifying (absorbing) medium," *Sov. Phys. Usp.*, vol. 12, pp. 641-672, 1970.
[14] E. Fill and W. Schmid, "Amplification of short pulses in CO_2 laser amplifiers," *Phys. Lett.*, vol. 45A, pp. 145-146, 1973.
[15] N. J. Frigo, "Ultrashort pulse propagation in saturable media: A simple physical model," *IEEE J. Quantum Electron.*, vol. QE-19, pp. 511-519, 1983.
[16] A. E. Siegman, *Lasers*. Mill Valley, CA: University Science, 1986, ch. 10.
[17] A. J. Lowery, "Explanation and modelling of pulse compression and broadening in near-travelling-wave laser amplifiers," *Electron. Lett.*, vol. 24, pp. 1125-1126, 1988.
[18] ——, "New inline wideband dynamic semiconductor laser amplifier model," *IEE Proc.*, vol. 135, pt. J, pp. 242-250, 1988.
[19] E. Schöll, "Dynamic theory of picosecond optical pulse shaping by gain-switched semiconductor laser amplifiers," *IEEE J. Quantum Electron.*, vol. 24, pp. 435-442, 1988.
[20] N. A. Olsson and G. P. Agrawal, "Spectral shift and distortion due to self-phase modulation of picosecond pulses in 1.5-μm optical amplifiers," *Appl. Phys. Lett.*, vol. 55, pp. 13-15, June 1989.
[21] G. P. Agrawal and N. K. Dutta, *Long-Wavelength Semiconductor Lasers*. New York: Van Nostrand Reinhold, 1986, ch. 2.
[22] C. H. Henry, "Theory of the linewidth of semiconductor lasers," *IEEE J. Quantum Electron.*, vol. QE-18, pp. 259-264, 1982.
[23] M. Osiński and J. Buus, "Linewidth broadening factor in semiconductor lasers—An Overview," *IEEE J. Quantum Electron.*, vol. QE-23, pp. 9-29, 1987.
[24] See, for example, Y. R. Shen, *The Principles of Nonlinear Optics*. New York: Wiley, 1984, pp. 325-329.
[25] G. P. Agrawal, *Nonlinear Fiber Optics*. Boston, MA: Academic, 1989.
[26] G. P. Agrawal and M. J. Potasek, "Effect of frequency chirping on the performance of optical communication systems," *Opt. Lett.*, vol. 11, pp. 318-320, 1986.
[27] N. A. Olsson, G. P. Agrawal, and K. W. Wecht, "16 Gbit/s, 70 km, pulse transmission by simultaneous dispersion and loss compensation with 1.5 μm optical amplifiers," *Electron. Lett.*, vol. 25, pp. 603-605, 1989.
[28] G. P. Agrawal and N. A. Olsson, "Amplification and compression of weak picosecond optical pulses by using semiconductor laser amplifiers," *Opt. Lett.*, vol. 14, pp. 500-502, 1989.

Govind P. Agrawal (M'83-SM'86) was born in Kashipur, India, on July 24, 1951. He received the M.S. and Ph.D. degrees in physics from the Indian Institute of Technology, New Delhi, in 1971 and 1974, respectively.

After spending several years at the Ecole Polytechnique, Palaiseau, France, the City University of New York, New York, and Quantel, Orsay, France, he joined AT&T Bell Laboratories, Murray Hill, NJ, in 1982 as a member of the technical staff. Since January 1989 he has been with the Institute of Optics, University of Rochester, Rochester, NY. His research interests have been in the fields of quantum electronics, nonlinear optics, and laser physics. He is an author or coauthor of more than 100 research papers and books entitled *Long-Wavelength Semiconductor Lasers* and *Nonlinear Fiber Optics*. He is currently engaged in the research and development of semiconductor lasers.

Dr. Agrawal is a member of the American Physical Society and a Fellow of the Optical Society of America.

N. Anders Olsson was born in Solleftea, Sweden, on April 13, 1952. He received the "Civilingenjorsexamen" degree in engineering physics from Chalmers University of Technology, Gothenburg, Sweden, in 1975, and the M.Eng. and Ph.D. degrees in electrical engineering from Cornell University, Ithaca, NY, in 1979 and 1982, respectively.

Between 1975 and 1977 he was with the Schlumberger Overseas SA, Singapore, as a Field Engineer assigned to the Far East Asian region. After six months as a Post-Doctoral Research Associate at Cornell University, he joined Bell Laboratories in 1982. His research interests include semiconductor lasers for optical communication, especially single-frequency sources.